Zeitschrift: Eclogae Geologicae Helvetiae
Herausgeber: Schweizerische Geologische Gesellschaft
Band: 73 (1980)
Heft: 1

Artikel: Mechanical aspects of the Jura overthrust
Autor: Müller, Walter H. / Briegel, Ueli
DOI: https://doi.org/10.5169/seals-164952

Eclogae geol. Helv.	Vol. 73/1	Pages 239-250	3 figures in the text and 1 table	Basle, March 1980

Mechanical aspects of the Jura overthrust[1])

By WALTER H. MÜLLER and UELI BRIEGEL[2])

ABSTRACT

Two hypotheses of Jura mountain building are discussed. Both are based on a decollement horizon underneath Jura, Molasse basin and a part of the Alps. The most likely lubricating material is anhydrite. A number of triaxial test runs with different types of anhydrite from Switzerland indicated that the flow strength of fine grained samples is clearly lower than that of coarse grained at slow strain rates and elevated temperature. This result is supported by thin-section studies on anhydrite of the wild cat Altishofen (Luzern) where fine-grained domains show flow structures and coarse-grained domains do not. The experimental data also led to a flow law of the power law type, which allows i.e. to determine the flow strength for distinct temperature and strain rate values. Both hypotheses have been approached by finite-element methods. The so-called Fernschub hypothesis (LAUBSCHER 1961), mainly gravity sliding plus an additional push from the southeast, could not reasonably be modelled, whereas the underthrust hypothesis (HSÜ 1979) seem to work without major mechanical problems.

ZUSAMMENFASSUNG

Zwei verschiedene Hypothesen zur Jurafaltung werden einander gegenübergestellt. Beide benötigen einen Abscherungshorizont in der Trias zwischen Jura und Alpen. Triaxial-Experimente bei erhöhter Temperatur und langsamer Verformungsgeschwindigkeit an Anhydrit, dem wahrscheinlichsten Gleitmaterial, ergaben eine deutlich tiefere Fliessfestigkeit bei feinkörnigem Material. Auch Dünnschliffe aus dem Anhydrit der Bohrung Altishofen (Luzern) zeigen Fließstrukturen nur in feinkörnigen Partien. Aus den Resultaten dieser Experimente liess sich auch ein exponentielles Fliessgesetz ableiten, welches z. B. erlaubt, die zu erwartende Fliessfestigkeit bei gegebener Temperatur und Verformungsrate zu bestimmen. Unter diesen Voraussetzungen war es möglich, die beiden Hypothesen mittels der Methode der finiten Elemente anzugehen. Es zeigte sich dann, dass die Fernschubhypothese (LAUBSCHER 1961) mechanisch grosse Probleme aufwirft, die Unterschiebungshypothese (HSÜ 1979) aber im Bereich des «Machbaren» liegt.

Introduction

Over the years a whole range of solutions of the origin of the fold-and-thrust belt of the Jura mountains have been proposed. At one end of the spectrum is the "Fernschub hypothesis" proposed by BUXTORF in 1907 and the assumption of a very plastic layer within the detachment horizon. LAUBSCHER (1961) suggested that it is possible to transmit the gravitational force of the Alpine nappe piles through the relatively undisturbed Molasse basin in a manner which could fold up the Jura and thus shorten the sedimentary cover for 10–20 km. The crystalline basement is not involved in this shortening process. Another interesting hypothesis has been

[1]) Contribution No. 147 of the Laboratory of Experimental Geology, ETH.

[2]) Geologisches Institut, ETH-Zentrum, CH-8092 Zürich.

proposed by PAVONI (1961). He extended the idea of several earlier authors (e.g. VONDERSCHMITT 1942) and postulated the existence of a series of wrench faults in the basement as responsible for the SSW-NNE "en échelon" grouping of the Jura folds. In this model a ductile detachment horizon was also assumed. The geometrical modelling simulates the actual fold and fault pattern of the Jura. However, the necessary basement fault system has been demonstrated in any of the regions. A third school of thought was advanced by UMBGROVE (1948). TRÜMPY (1960) and more recently revived by HSÜ (1979) postulated underthrusting basement under the Aar massif, and not under the Molasse, as UMBGROVE did. Basically this is a variation of the "Fernschub" hypothesis, but with significantly different boundary conditions.

The accumulation of knowledge during the past several years concerning the detachment horizon, the flow behavior of the lubricating anhydrite and the development of methods for calculating the stability and stress distribution in multilayer models have allowed us to test these different models on the origin of the Jura mountains. All models assume a very ductile material with little flow strength between the sedimentary cover and basement. Therefore we shall deal first with this major problem.

The gliding material of the detachment horizon

Evaporites are known to play an important role as gliding material in different decollement zones (HEARD & RUBEY 1966). In the absence of rock salt, anhydrite is the most likely and usually abundant gliding material, as gypsum was not stable and was probably not in existence under the conditions of decollement gliding. Sulfate has either apparently been precipitated as anhydrite or has been diagenetically altered to anhydrite because of its deep burial (MACDONALD 1953; HARDIE 1967). Further, no drill hole report nor core sample studies give any indication for unusual water pressures within the Triassic strata underneath the Molasse today, which might reduce the strength of the gliding layer as HEARD & RUBEY (1966) speculated. Extensive experimental work on anhydrite (MÜLLER & BRIEGEL 1977, 1978) revealed the following behavior: fine-grained anhydrite deformed at high temperature and slow strain rate has a significantly lower creep strength than coarse-grained material. Interpretation of the drill cores from the Keuper in the Altishofen borehole at 2100 m depth are in accordance with this result: Intensive deformation and shearing has been observed in zones where the anhydrite is fine-grained, and no indication of deformation took place in coarse-grained anhydrite. Microscopic studies suggest dislocation creep to be the dominant deformation mechanism. Generation of subgrains leads to a certain polygonization of the grain structure. In experimentally deformed samples this mechanism dominates in the low stress field (Fig. 1). The concordance of the field and laboratory investigations suggest that the decollement horizon lies within fine-grained anhydrite which was subjected to deformation at high temperature and slow strain rate.

Sample logs of the boreholes Courtion I and Altishofen by FISCHER & LUTERBACHER (1963) show clearly several deformed layers within the "Anhydrit-Gruppe" and "Gips-Keuper". The decollement zone there consists of a number of shear horizons of heavily deformed fine-grained anhydrite within a few hundred meters of

Triassic strata. The overall deformation within the decollement zone seems to have operated in a card-deck simple-shear manner. We believe that fine-grained anhydrite was the lubricant material over the major area of overthrust. However, wherever rock salt is present, it will act as lubricant. Also shales may play a significant role in this deformation process, especially where the pore pressure exceeded the hydrostatic value.

Experiments

A large number of triaxial deformation tests have been performed in order to get the flow strength of fine-grained anhydrite as a function of depth, temperature and strain rate. Apparatus and experimental techniques have been described earlier (MÜLLER & BRIEGEL 1977, 1978). For sample material we chose a very pure, fine-grained anhydrite from a recent drill hole in the Jura (NAGRA-Bohrung 4, Wandflue, depth 72.7–73.5 m), as listed in MÜLLER & BRIEGEL (1977, p. 696). The grain size 0.01–0.5 mm corresponds approximately to the one from the Altishofen mylonite.

All our cylindrical specimen were deformed in compression at a confining pressure of 1.5 kbar. Three different test procedures have been applied:

Constant strain rate tests, dry and with pore pressure

Our apparatus is not a very stiff one, resulting in slightly different strain rates for the elastic and plastic portion of one test. In most of our experiments a constant flow

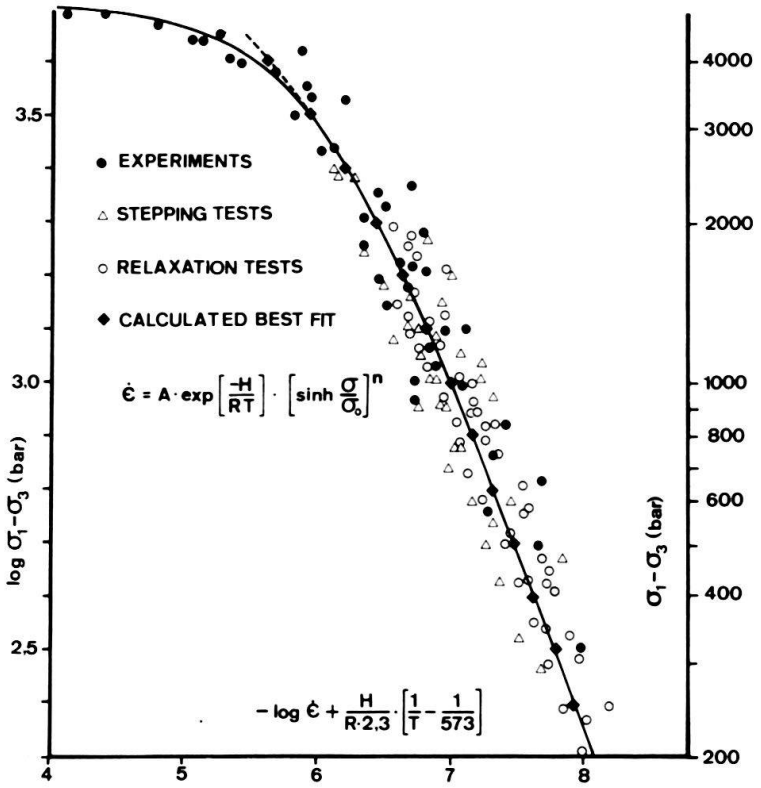

Fig. 1. Data of the Table homologized to 300 °C. The black dots represent the constant strain rate results at 10% strain, the open circles the stress relaxation values and the open triangles values of the stepping tests.

Table: *Deformation tests on fine-grained anhydrite at 1.5 kbar confining pressure (R = stress relaxation tests, S = stepping tests).*

Temperature °C	Differential stress at 10% strain (bar)	Strain rate sec^{-1}	Experiment Nr
450°	2130	$8,3.10^{-5}$	AWP 58 R
450°	1610	$2,3.10^{-5}$	AWP 87 S
450°	1510	$3,1.10^{-5}$	AWP 93 S
450°	1400	$4,5.10^{-5}$	AWP 52
450°	1260 (5.9%)	$1,2.10^{-5}$	AWP 89 S
450°	1080	$2,0.10^{-5}$	AWP 53 R
450°	990	$1,2.10^{-5}$	AWP 54 R
450°	830	$5,7.10^{-6}$	AWP 55
450°	500	$3,3.10^{-6}$	AWP 56
450°	320	$1,5.10^{-6}$	AWP 57
400°	3190	$8,3.10^{-5}$	AWP 59
400°	2760	$4,3.10^{-5}$	AWP 60
400°	2030	$2,0.10^{-5}$	AWP 61 R
400°	1670	$1,1.10^{-6}$	AWP 86 S
400°	1640	$8,7.10^{-6}$	AWP 90 S
400°	1500	$1,2.10^{-5}$	AWP 62 R
400°	1250	$4,0.10^{-6}$	AWP 65
400°	1160	$5,2.10^{-6}$	AWP 63
400°	730	$1,6.10^{-6}$	AWP 64
350°	4390	$7,7.10^{-5}$	AWP 66
350°	4070	$4,1.10^{-5}$	AWP 67
350°	3840	$1,8.10^{-5}$	AWP 68
350°	3570	$1,1.10^{-5}$	AWP 69
350°	3400	$5,4.10^{-6}$	AWP 70
350°	2350	$1,7.10^{-6}$	AWP 71
350°	2030	$3,9.10^{-6}$	AWP 72
350°	1900	$1,2.10^{-6}$	AWP 85 S
350°	1690 (λ=0,9)	$6,0.10^{-7}$	AWλ 2
350°	1570	$2,3.10^{-6}$	AWP 88 S
350°	910 (λ=0,66)	$3,8.10^{-7}$	AWλ 1
350°	660	$1,5.10^{-7}$	AWP 82
350°	580	$3,6.10^{-7}$	AWP 81
300°	4910	$4,1.10^{-5}$	AWP 75
300°	4900	$7,8.10^{-5}$	AWP 73
300°	4680	$1,8.10^{-5}$	AWP 76
300°	4470	$5,5.10^{-6}$	AWP 78
300°	4370	$7,8.10^{-6}$	AWP 77
300°	4210	$1,3.10^{-6}$	AWP 79
300°	3940	$3,7.10^{-6}$	AWP 80
300°	2720	$9,9.10^{-7}$	AWP 92 S
300°	1800	$4,5.10^{-7}$	AWP 83
300°	1000	$1,9.10^{-7}$	AWP 84

stress has been established very soon (1-2% strain), the main part of the deformation (8-9%) took place at constant strain rate conditions. Two experiments with pore pressure of $\lambda = 0.75$ and $\lambda = 0.9$ do not deviate appreciably from the dry experiments (Table). However, this mechanical behavior was caused by the fact that a pore pressure was not established as a consequence of pore-closing mechanisms. We have, therefore, to assume that we cannot deal with pore-pressure effects within the anhydrite shear zones at such a strain rate. A summary of all our experiments is compiled in the Table (strength at 10% strain).

Stepping tests

A regular constant strain rate test is started. Once the constant flow stress is established, the strain rate was changed for a certain period of time and afterwards again returned to the initial value. This change can be repeated several times with different step intervals. This procedure helps to save much laboratory time, as the strain rate dependence of the tested material (at a given temperature and confining pressure) is revealed in a single test run. The data points of these tests (triangles) fit nicely into the other data sets of Figure 1.

Relaxation tests

With this technique, described e.g. in MÜLLER & BRIEGEL (1978), we get stress-strain data for a large variety of strain rates at the end of any regular constant strain rate test, when the elastic energy stored in the apparatus and in the sample is slowly converted into plastic deformation of the sample. Relaxation test points help us greatly to extend the range of data down into the low stress, slow strain rate field (open circles in Fig. 1). All the experiments plotted in Figure 1 are carried out at different temperatures, but have been homologized to 300 °C. This is allowed because the activation energy observed over the range of conditions remained approximately constant.

The flow law

The experimental data have been treated in exactly the same way as in our 1978 paper. Again the activation energy (H) for creep was basically independent of temperature and strain rate. Because of excessive work hardening, data points with differential stresses above 4.0 kbar have been omitted as well as the two pore pressure runs for reasons of compatibility. The activation energy has been calculated for small stress intervals ($\Delta \log \sigma = 0.005$) with the respective stress, temperature and average strain rate, to be 27.3 ± 2.6 kcal·mol^{-1} and was found to be also independent of stress. All the data of the Table (with exceptions as above) have been normalized to a temperature of 300 °C and plotted in Figure 1. Thus the data points gather along a smoothly bent curve which seems to straighten towards the low stresses. The calculated best fit satisfies nicely the flow law:

$$\dot{\varepsilon} = A \cdot \exp\left(\frac{-H}{RT}\right)\left(\sinh\frac{\sigma}{\sigma_0}\right)^n$$

where $\dot{\varepsilon}$ is the strain rate, A, σ_o and n are constants, R is the gas constant, and T is the temperature in °K. For our Wandflue anhydrite the constants have been determined to be: $A = 6025.6\ \text{sec}^{-1}$, $H =$ as above, $\sigma_o = 1.7$ kbar, $n = 1.5$.

This flow law, as may be taken from Figure 1, is only good up to a differential stress of 3.5 kbar. At higher stresses work hardening becomes significant and the strength becomes highly dependent on confining pressure.

Thin-section studies

The textures of our deformed samples show remarkable differences depending on the conditions they have experienced. If the differential stress exceeds 3.5 kbar, distinct cataclasis is observed. At lower values, intracrystalline mechanisms such as twinning and probably also dislocation glide dominate. Below 1.5 kbar starts the development of subgrains and the grain boundaries become frayed, strong indications for dislocation creep. Grain-boundary sliding does not seem to occur abundantly although it is expected to operate at these low stresses and at a power $n = 1.5$ in our flow law, if compared to limestone deformation. The extremely low activation energy (27.3 $\text{kcal} \cdot \text{mol}^{-1}$, only rock salt is lower with 23.5 $\text{kcal} \cdot \text{mol}^{-1}$), may be responsible for this deformation behavior, which is different from that of a limestone.

Strain rate and temperature assumptions

Strain rate and temperature are the main parameters to influence the flow strength of the gliding material. Therefore, it is essential to evaluate the best possible values.

The geological timing of the folding phase or phases is still problematic. Stratigraphic-tectonic bracketing led us to assume a time span of 8 million years (Hipparion sands, Sundgauschotter). With this number, a mean decollement zone thickness of 100 m and an average shortening of the detached sediment pile of 15 km we calculated a strain rate of $6 \times 10^{-13}\ \text{sec}^{-1}$ which corresponds to an overthrust velocity of roughly 2 mm per year. This displacement is comparable to the 3 mm/yr rate obtained by HSÜ (1979) for the Jura movement.

A series of heat flow measurements in different Swiss lakes (VON HERZEN et al. 1974; FINCKH 1976 and pers. comm.) suggest a rather high geothermal gradient of about 50 °C/km. Borehole measurements (RYBACH et al. 1978), however, indicate much lower values between 30 and 40 °C/km. There seems to be a systematic discrepancy between the two sets of data. To make our calculations, we used a value of $40\ ^\circ\text{C} \cdot \text{km}^{-1}$ and a surface temperature of 10 °C.

The finite element models

The application of the finite element method to Geology has been discussed by several authors (e.g. DIETRICH & CARTER 1969; VOIGHT & SAMUELSON 1969; BOCK 1972; MÜLLER & HSÜ 1980). For the following considerations we used the computer program STAUB (Statistische Analyse von Untertags-Bauten) developed at the Civil Engineering Department of ETH Zürich (KOVARI 1969) based on the fun-

damental work of ZIENKIEWICZ et al. (1967, 1969). The STAUB program assumes an elastic-ideally plastic behavior of the stressed medium, i.e. while one part of the system is elastically strained, the rest may be plastically deformed. In the plastic part, the strain includes an elastic and a plastic increment. Local plastic regions are bounded by regions which remain elastic and the boundary conditions are set to prevent an unlimited plastic flow. The program also uses the yield criterion of DRUCKER & PRAGER (1952), which corresponds to the Mohr-Coulomb-Navier criterion in two-dimensional problems, and therefore is also related to the Mohr-Coulomb criterion for fracture (JAEGER 1969). In other words this criterion is valid as an expression of the fracture criterion for brittle, and also as the yield stress for ductile deformation (HSÜ 1969; HANDIN 1969).

The first model by LAUBSCHER of the rotational sliding type (Fernschub) is simulated by a cross section from the Alps through the Molasse basin to the Jura (Fig. 2*a*). To compensate for the maximum possible erosion since the time of overthrusting, we accounted for an extra 500 m of Molasse and up to 4000 m of limestone above the present topography of the Alps. This finite element model is divided into 596 elements and 341 nodal points. The size of the elements was gradually reduced from the base and from the surface towards the decollement zone, which is about 100–200 m thick. In this model (model 1A) we simulated gravity sliding only by a rotation of the mass, without an additional push from the south. For the simulation computations we assigned the Mohr-Coulomb criterion for failure to rocks outside the gliding zone and our empirical flow law for plastic yielding to the anhydrite within the gliding zone. Where the stress difference is less than the critical shear stress or the creep strength, the response was elastic and where the stress difference became greater, the response of the respective element was plastic deformation. To simplify the problem, only three different rock types were chosen: anhydrite as decollement zone, limestone above it and granite below it. On the basis of available experimental data (CLARKE 1966; MÜLLER & BRIEGEL 1977) the following material properties have been selected:

	Granite	Anhydrite	Limestone
Young's modulus E	800 kbar	250 kbar	600 kbar
Poisson's ratio	0.3	0.3	0.3
Density	2.6 g/cm^3	2.9 g/cm^3	2.6 g/cm^3
Cohesive strength	800 bar	400 bar	970 bar
Coefficient of internal friction	40°	30°	24°

The detachment horizon induced by boundary displacement is defined by the criterion that the stress at an element in the gliding zone is greater than the differential stress required for creep at the temperature (i.e. depth) and strain rate assumed for that element. The results show that the detachment horizon could only be developed up to the region of Burgdorf (km 68). No other elements of the model satisfied the flow or fracture conditions, especially not in the region of the Jura mountains, where there should be a zone of instability to induce folding by brittle rock deformation and pressure solution (LAUBSCHER 1961, 1979). This brought us to the conclusion that the shear force produced by gravity sliding was not even sufficient to produce the required decollement horizon, not to mention the folding of the Jura mountains.

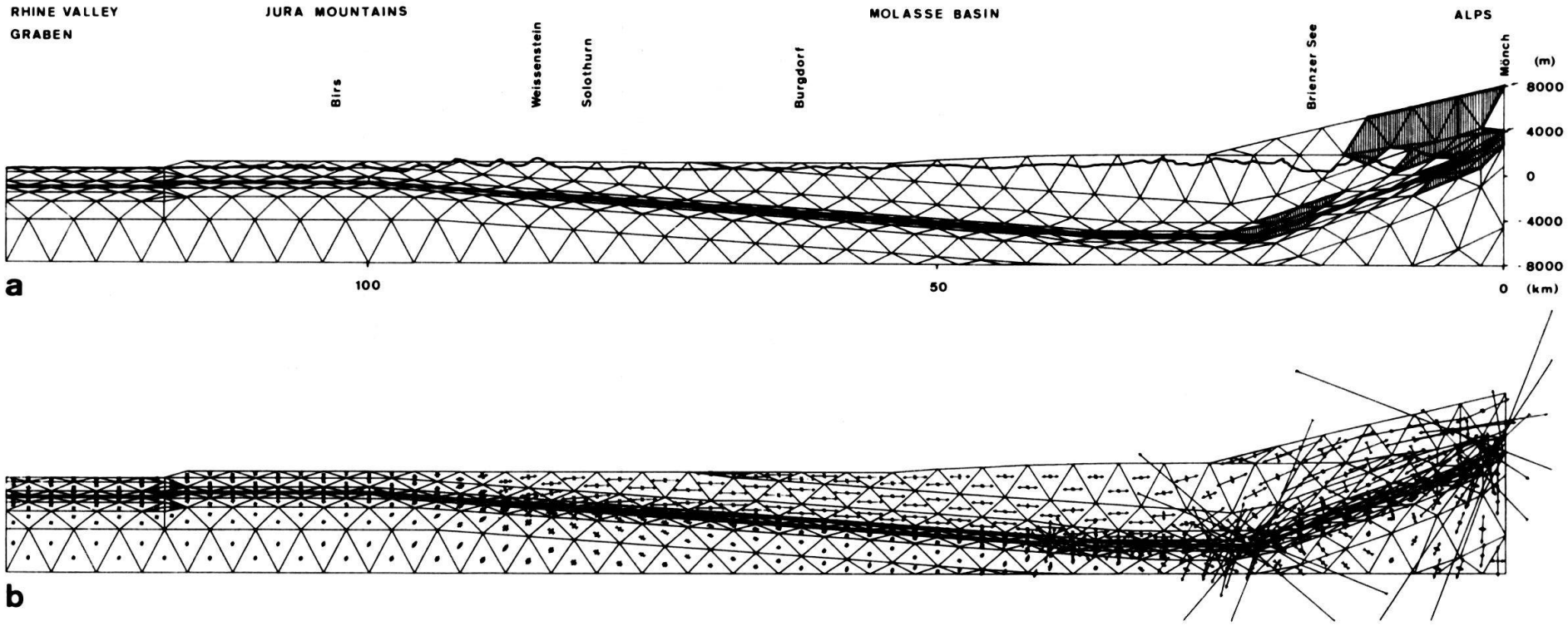

Fig. 2. The finite element model simulating the "distant-push" model (model 1, variant B). The cross-section stretches from the Alps through the Molasse basin and the Jura mountains to the Rhine Graben. The stresses were produced by gravity gliding caused by the unequal distribution of masses on the concave detachment horizon and by additional push (displacement $u = 170$ m, $v = 40$ m) from the Alps.

a: The heavy line shows the development of the ductile decollement horizon and the vertical hatched area shows the region of instability.

b: Stress distribution in the model 1, variant B. The arrows show the direction of principal stresses and the length of arrows gives a measure of magnitude (1 mm = 3.3 kbar).

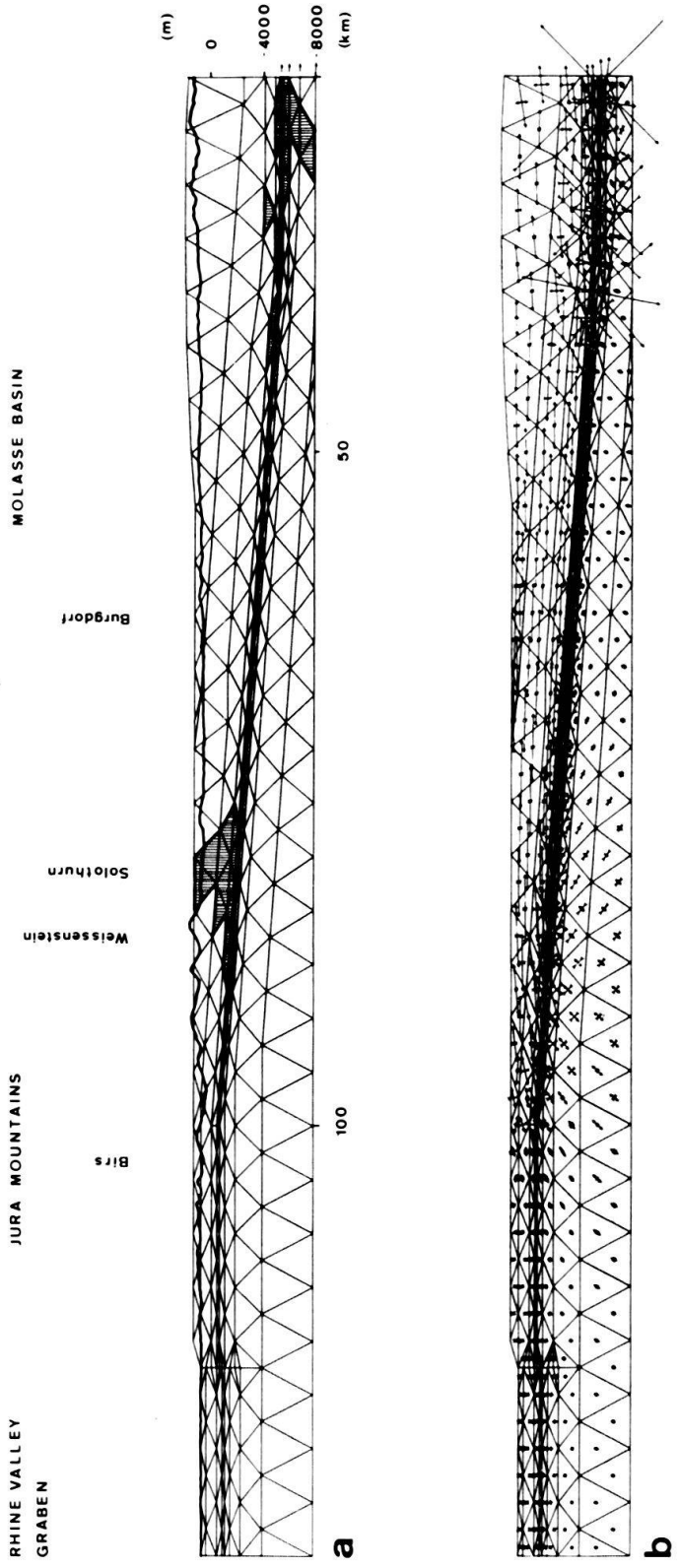

Fig. 3. The finite-element model simulating the underthrusting model (model 2).

a: The arrows show the direction of underthrusting (displacement $u = 225$ m, $v = 0$). The heavy line shows the development of ductile detachment horizon and the vertical hatched area shows region of instability.

b: Stress distribution of model 2.

The variation of the rotational sliding model (model 1B) is similar to the first one but with an additional push from the Alps (Fig. 2*a* and *b*, indicated by small arrows in *a*). Now the detachment horizon could be developed up to the region beneath the Jura mountains (km 88). However, Figure 2*a* shows two zones of instability within the rotational slab. The first one in the Alps where the push is applied and the second one at the deepest portion of the slab above the detachment horizon. On the other hand, a zone of instability has not been developed within the region of the Jura mountains. In other words, the force to generate a long enough detachment horizon would result in yielding of the overthrust block long before the stress could be transmitted to induce the folding of the Jura mountains.

In the second model we simulated an underthrusting of the crystalline basement under the Aar massif. For computer time saving reasons, the finite element model has been shortened and starts at km 22, the beginning of the underthrust; the portion further south would not have been affected at all. For this arrangement, the whole model was displaced from left to right whereby the right hand edge was kept fixed except for the four lowest nodal points (Fig. 3*a*, *b*), which were allowed to move to the right also. The anhydrite of the detachment layer proved to be unstable up to a boundary well within the region of the Jura mountains (km 98). Further north, the detachment horizon approaches too much the surface and the material properties of anhydrite change towards those of limestone (MÜLLER & BRIEGEL 1978). In addition we got two areas of instability within the thrust-plate above the detachment horizon. The first one in the south, where crystalline basement is being underthrust under the massif and another one in front of the Jura near Solothurn. The Molasse basin remains essentially stable.

Discussion

The finite element program STAUB allows it to be demonstrated that large overthrusts are unlikely within a homogeneous body. One or more weak layers are needed in order to develop a detachment horizon or zone (MÜLLER & HSÜ 1980). Under the Jura mountains the weak layer consists of evaporites and shales with several very fine grained anhydrite beds. Three different models of Jura overthrusting have been calculated.

The first model (1A) assumed deformation of the Jura mountains by rotational gliding of the first slab through gravity caused by the unequal distribution of masses on a concave detachment horizon underneath the Alps, Molasse basin and the Jura. The result shows the mechanical infeasibility of this assumption: a decollement horizon cannot be developed under the Jura mountains, even if the Alps were as high as the Himalayas today.

An alternative of the rotational gliding model (1B, see Fig. 2) introduces an additional push from the Alps. A detachment horizon could be extended to the region of the front range of the Jura. However, a first area of instability was created in the Alps at the southern end of the slab, where the extra push was applied. Due to the overload of up to 8000 m of overburden, the lubricating layer becomes so weak that all the gravitational force and the extra push are fully concentrated at the morphologic deepest part of the decollement track and led there to stresses exceed-

ing the failure strength, generating an instability which prevents continuation of overthrusting. Thus the stress could not be transmitted to cause the Jura deformation.

A good result was obtained with the model (2) of underthrusting the basement under the Aar massif. A detachment horizon was developed far into the Jura mountains. Enough shear stress could be transmitted through the Molasse to induce instability and some deformation in the Jura, while the Molasse basin remained stable. The now formed instability area in front of the Jura is regarded as an important result of this model. The detachment horizon continues to develop far beyond the zone of instability underneath the Jura mountains, whereas at the same time one branch breaks through this zone to reach the surface. This feature may correspond to the actual separation of the Folded Jura and the Table Jura, although the location of the branching off in the model does not exactly correspond to that in nature. The instability zone allows the detachment horizon to diverge upwards as a thrust by brittle fracture. Simultaneously a small part of the displacement continues underneath the Table Jura by ductile deformation and may be responsible for the minor folding in that region and for the overriding of the Jura beyond the Rhine- and Bresse-Graben edge. The fact, that the simulated branching off of the lubricating layer does not take place at the expected spot and also that the simulated detachment horizon does not reach as far as the Rhine Graben are probably due to the simplification we had to apply to our model and as well to the still somewhat problematic values for the physical properties, temperature and strain rate we had to plug into our calculations. A slightly higher geothermal gradient at the time of overthrusting, an appreciable role attributable to rock salt within the decollement zone or a slower strain rate should shift the instability to the northwest and thus produce a model in closer similarity to the actual situation. The peculiar arched shape of the Jura cannot be solved with this two-dimensional method. However, if we allow for wrench faults in the basement as proposed by PAVONI (1961), we think that a solution is possible. As a matter of fact, several almost vertical faults have been detected by drilling for oil, especially in the French part of the Jura.

Acknowledgment

We would like to thank the staff of the Civil Engineering Department of ETH Zürich for permission to use the STAUB program. We are particularly indebted to Mr. K. Kovari for many helpful discussions. Valuable help from and discussions with K.J. Hsü, R. Trümpy, A.G. Milnes, H. Bürgisser, U. Gerber, and K. Ghilardi contributed to this work.

REFERENCES

BOCK, H. (1972): *Vielfache Bruchstrukturen bei einfachen Beanspruchungen.* - Geol. Rdsch. *61*/3, 824–849.

BUXTORF, A. (1907): *Geologische Beschreibung des Weissenstein-Tunnels und seiner Umgebung.* - Beitr. geol. Karte Schweiz [N.F.] *21*.

CLARK, S.P. (1966): *Handbook of Physical Constants.* - Mem. geol. Soc. Amer. *97*, 587 p.

DIETRICH, J.H., & CARTER, N.L. (1969): *Stress History of folding.* - Amer. J. Sci. *267*, 129–154.

DRUCKER, D.C., & PRAGER, W. (1952): *Soil mechanics and plastic analysis limit design.* - Quart. appl. Math. *10*, 157–165.

FINCKH, P. (1976): *Wärmeflussmessungen in Randalpenseen.* - Diss. ETH Zürich, No. 5787.

FISCHER, H., & LUTERBACHER, H. (1963): *Das Mesozoikum der Bohrungen Courtion I und Altishofen 1.* - Beitr. geol. Karte Schweiz [N.F.] *115.*

HANDIN, J. (1969): *On the Coulomb-Mohr failure criterion.* - J. geophys. Res. *74*/22, 5343-5348.

HARDIE, L.A. (1967): *The gypsum-anhydrite equilibrium at one atmosphere pressure.* - Amer. Mineralogist *52*, 171-200.

HEARD, H.C., & RUBEY, W.W. (1966): *Tectonic implications of gypsum dehydration.* - Bull. geol. Soc. Amer. *77*, 741-760.

HSÜ, K.J. (1969): *Statics and kinetics of the Glarus overthrust.* - Eclogae geol. Helv. *62*/1, 143-154.

— (1979): *Thin-skinned plate tectonics during Neo-alpine Orogenesis.* - Amer. J. Sci. *279*, 353-366.

JAEGER, J.C. (1969): *Elasticity, fracture, and flow.* - Methuen, London.

KOVARI, K. (1969): *Ein Beitrag zum Bemessungsproblem von Untertagbauten.* - Schweiz. Bauztg. *87.*

LAUBSCHER, H.P. (1961): *Die Fernschubhypothese der Jurafaltung.* - Eclogae geol. Helv. *54*/1, 221-282.

— (1979): *Jura kinematics and dynamics.* - Eclogae geol. Helv. *72*/2, 467-483.

MACDONALD, G.J.F. (1953): *Anhydrite-Gypsum equilibrium relations.* - Amer. J. Sci. *251*, 884-898.

MÜLLER, W.H., & BRIEGEL, U. (1977): *Experimentelle Untersuchungen an Anhydrit aus der Schweiz.* - Eclogae geol. Helv. *70*/3, 685-699.

— (1978): *The rheological behavior of polycrystalline anhydrite.* - Eclogae geol. Helv. *71*/2, 397-407.

MÜLLER, W.H., & HSÜ, K.J. (1980): *Stress distribution in overthrusting slabs and mechanics of Jura deformation.* In: Stresses in the Alpine-Mediterranean region. - Springer-Verlag, Wien.

PAVONI, N. (1961): *Faltung durch Horizontalverschiebung.* - Eglogae geol. Helv. *54*/2, 516-534.

RYBACH, L., BODMER, P., PAVONI, N., & MÜLLER, ST. (1978): *Sit Criteria for Heat Extraction from Hot Rock.* - Pageoph *116*, 1211-1224.

TRÜMPY, R. (1960): *Paleotectonic evolution of the central and western Alps.* - Bull. geol. Soc. Amer. *71*/6, 843-908.

UMBGROVE, J.H.F. (1948): *Origin of the Jura Mountains.* - Proc. (k.) nederl. Akad. Wetensch. *51*, 1049-1062.

VOIGHT, B., & SAMUELSON, A.C. (1969): *On the application of finite-element technique to problems concerning potential distribution and stress distribution analysis in the Earth Sciences.* - Pure and appl. Geophys. *76*, 40-55.

VONDERSCHMITT, L. (1942): *Die geologischen Ergebnisse der Bohrungen von Hirtzbach bei Altkirch (Ober-Elsass).* - Eclogae geol. Helv. *35*/1, 67-99.

VON HERZEN, R.P., FINCKH, P., & HSÜ, K.J. (1974): *Heatflow Measurements in Swiss lakes.* - J. Geophys. *40*, 141-172.

ZIENKIEWICZ, O.C., & CHEUNG, Y.K. (1967): *The finite element method in structural and continuums mechanics.* - McGraw-Hill, New York.

ZIENKIEWICZ, O.C., VALLIAPAN, S., & KING, J.P. (1969): *Elastoplastic solutions of engineering problems' initial stress; finite element approach.* - Int. J. num. Meth. Eng. *1*, 75-100.